Available online at www.sciencedirect.com

SciVerse ScienceDirect

Ceramics International 38 (2012) 4065–4074

CERAMICS INTERNATIONAL

www.elsevier.com/locate/ceramint

Processing and properties of sol gel derived alumina–carbon nano tube composites

Sophia Rani Inbaraj [a,*], Reeta Mary Francis [b], N. Victor Jaya [a], Anil Kumar [c]

[a] Department of Physics, College of Engineering, Anna University, Chennai, Tamil Nadu 600025, India
[b] Department of Physics, Government Arts College, Coimbatore, Tamil Nadu 641018, India
[c] Advanced Systems Laboratory, Research Centre Imarat, Hyderabad, Andrapradesh 500069, India

Received 8 September 2011; received in revised form 23 January 2012; accepted 24 January 2012
Available online 5 February 2012

Abstract

High purity alumina–carbon nano tube (CNT) composites were prepared by an aqueous sol–gel processing route. CNTs were dispersed in alumina sol containing appropriate amount of MgO precursor. Aqueous slurry of alumina was seeded into the sol followed by gelation, drying and calcination at 1000 °C for 1 h. The calcined powder consisting of alumina-coated CNTs and alumina was milled, sieved, dried, pressed and pressureless sintered at 1400–1600 °C for 1 h in nitrogen atmosphere. Sintered samples were further isostatically hot pressed at 1300 °C and the properties were compared with the pressureless sintered samples. Phase formation was followed by XRD study, CNT retention was confirmed by Raman studies and the samples were further characterized for mechanical and microstructural properties.

Keywords: A. Sintering; A. Hot isostatic pressing; B. Composites; Alumina–CNT; Sol gel

1. Introduction

Carbon nano tubes (CNTs) are exceptionally flexible during bending and show substantial promise for structural applications [1]. The combination of high strength, extraordinary flexibility and resilience characteristics of CNTs can be utilized to enhance the fracture toughness of structural ceramics (for e.g., alumina) by dispersing appropriate quantity of CNTs in the base alumina matrix. However, achieving dense alumina composite with uniform CNT distribution is intricate due to the intrinsic characteristics of CNTs such as clustering and poor wetting behaviour with the matrix. These characteristics of CNTs result in heterogeneous distribution and poor reinforcing effect of CNTs in the final product. Moreover, strong processing conditions such as acid treatment during purification and surface treatment of CNTs, high energy milling or prolonged sonication during dispersion, high temperature and pressure during consolidation may also lead to the structural damage of CNTs [2] resulting in deterioration of the final properties of the composite.

Hitherto, several researchers have attempted to disperse CNTs in alumina matrix by various processes such as direct mixing of CNTs with alumina powder with [3,4] and without a non aqueous medium [5], in situ synthesis of CNTs on alumina powder using CVD technique [6–8], colloidal processing in which the appropriate charges were introduced on CNTs and alumina for optimal dispersion [9], molecular level mixing of functionalized CNTs in aluminium nitrate solution followed by oxidation [10], mixing of CNTs in alumina sol followed by gelation and calcination [11], deposition of polymer ultra thin films on CNTs and alumina by plasma polymerization [12], hydro thermal synthesis of boehmite [13,14] on CNTs etc. Moreover surface modification of CNTs by acid treatment [10] and use of surfactants [15–17] have been adapted to improve the dispersion of CNTs in alumina matrix. Consolidation techniques such as conventional pressureless sintering [3,12,18], hot pressing [8,13,16,17] and spark plasma sintering [4,5,7,10,11,14,19,20] were generally used for the fabrication of alumina CNT composites. Based on the degree of dispersion and densification achieved, the fracture toughness of CNT–alumina composites varied from −35% [15] to +300% [19] with respect to the fracture toughness of pure alumina samples.

* Corresponding author.
E-mail address: sophiarani@gmail.com (S.R. Inbaraj).

0272-8842/$36.00
doi:10.1016/j.ceramint.2012.01.064

Table 1
Overview of best mechanical properties achieved in alumina CNT composites through various processing methods.

Alumina characteristics	CNT characteristics	Mixing methods	Consolidation and sintering	Mechanical properties	Ref.
α-Al_2O_3 grain size – 0.5 μm	CVD-MWCNTs, 1.5 vol%, 98% purity, diameter (Φ): 5–20 nm, length(l): 2.5 μm	Ultrasonication, ball milling	Uniaxial pressing, CIPing, conventional sintering, 1550 °C, Argon	K_{IC}: 4.68 MPa $m^{1/2}$, flexural strength (σ_f): 202.3 MPa, % TD: 90	[3]
α-Al_2O_3 99.9% purity grain size – 0.5 μm	CVD-MWCNTs, 0–6 vol%, Φ: 10 nm, l: several μm	Ultrasonication, ball milling	SPS, 1400 °C, 50 MPa, vacuum	–	[4]
γ-Al_2O_3, particle size: 15 nm	Hipco-MWCNTs, 10 vol%	High energy dry ball milling	SPS, 1150 °C, 63 MPa, vacuum	K_{IC}: 9.7 MPa $m^{1/2}$, H_v: 1610 Kg/mm^2, % TD: 100	[5]
α-Al_2O_3 Φ: 30 nm	CVD-CNTs, 1.5 wt%	In situ CVD synthesis, 800 °C	SPS, 1300 °C, 55 MPa, Argon	K_{IC}: 6.3 MPa $m^{1/2}$, H_v: 20.1 GPa	[7]
α-Al_2O_3	CVD-MWCNTs, 4 wt%, Φ: 10–50 nm, l: 5–10 μm	In situ CVD synthesis	Hot pressing, 1800 °C, 40 MPa, Argon	H_v: 20 GPa friction coeff.: 0.45, wear loss: ~0.6 mg	[8]
Al_2O_3, Particle size: 200–300 nm	CVD-MWCNTs, 1 wt%, Φ: 10 nm, l: 100 nm	Colloidal processing	Hot pressing, 1350 °C, 30 MPa, Argon	K_{IC}: 4 ± 0.5 MPa $m^{1/2}$, σ_f: 536 ± 44 MPa	[9]
Source: aluminium nitrate	CVD-MWCNTs, 1.8 vol%	Molecular level mixing	SPS, 1500 °C, vacuum	$K_{IC}/K_{IC\ alumina}$: ~1.3 MPa $m^{1/2}$, H_v: 1550 Kg/cm^2	[10]
Source: aluminium tri-sec- butoxide	CVD-MWCNTs, 1.5 vol%, Φ: 15–30 nm, l: 10–50 μm	Sol–gel processing, powder calcination at 1200 °C	SPS, 1650 °C, 25 MPa	$K_{IC}/K_{IC\ alumina}$: ~1.11 MPa $m^{1/2}$, H_v: ~19.2 GPa	[11]
Al_2O_3, Φ: 47 nm	SWCNTs, 9 wt%, Φ: 1.3 nm, l: 0.5–3 μm	Ultrasonication and plasma polymerization	Sintering, 1000 °C in $H_2 + N_2$ mixture atm/hot pressing, 1200 °C, 120 MPa	Strength: 97.8 MPa, modulus: 9.85 GPa	[12]
Al_2O_3 particle size: 20 nm	CVD-MWCNTs, 5 wt%, Φ: 20–40 nm, l: 5–20 μm	Ultrasonication, hydrothermal crystallization, ball milling	Hot pressing, 1500 °C, 40 MPa, vacuum	K_{IC}: 5.87 MPa $m^{1/2}$, σ_f: 409.53 MPa, % TD: 97.4	[13]
Source: boehmite from basic aluminium acetate	MWCNTs, 1 wt%, Φ: 20 nm, l: 10–25 μm	Magnetic stirring, ultrasonication, hydrothermal synthesis	SPS, 1600 °C, 50 MPa	Hardness: 28.57 GPa, %TD: 98	[14]
Source: aluminium hydroxide	CVD-MWCNTs, Φ: 20–40 nm, l: 0.4–16.5 μm	Planetary centrifugal mixing with surfactant	SPS, 1500 °C, 20 MPa, vacuum	K_{IC}: ~4.1 MPa $m^{1/2}$, σ_f: ~325 MPa, % TD: 95	[15]
Al_2O_3 particle size: 200 nm, purity: > 99%	MWCNTs, 12 vol%	Ultrasonication with surfactant, ball milling	Hot pressing, 1500 °C, 20 MPa, Argon	K_{IC}: 5.55 ± 0.26 MPa $m^{1/2}$, σ_f: 314.4 ± 22.4 MPa, % TD: 95.4	[16]
Al_2O_3 particle size: 40 nm	CVD-CNTs, 2 wt%, Φ: 40 nm	Ultrasonication with surfactant	Hot pressing, 1600 °C, 40 MPa, vacuum	K_{IC}: 6.8 ± 0.3 MPa $m^{1/2}$, σ_f: 380 ± 18 MPa, H_v: 18 ± 0.3 GPa, % TD: 99.1	[17]
Al_2O_3, particle size: 500 nm, surface area: 3.75 m^2/g	MWCNTs, 1 vol%, Φ: 30–50 nm, l: 0.5–2 μm, >95% purity	Ultrasonication, milling, freeze drying	CIPing, 310 MPa, sintering, 1500 °C, Argon	K_{IC}: 4.1 ± 0.6 MPa $m^{1/2}$, σ_f: 543 ± 37 MPa, H_v: 22.3 GPa, % TD: 99	[18]
α-Al_2O_3 particle size: 150 nm	CVD-MWCNTs, 3.5 vol%, Φ: 20–70 nm	Colloidal processing	SPS, 1500 °C, 50 MPa, vacuum	K_{IC}: 5.2 MPa $m^{1/2}$, % TD: 99	[20]
Al_2O_3	SWCNTs, 1 wt%	Ultrasonication with surfactant, mechanical stirring	Hot pressing, 1600 °C, 20 MPa, Argon	K_{IC}: 6.4 ± 0.3 MPa $m^{1/2}$, σ_f: 423 ± 35 MPa	[21]
Al_2O_3	CVD-MWCNTs, 12 wt%, Φ: 10–50 nm, l: 3–5 μm. >95% purity	Ball milling, tape casting	Hot pressing, 1850 °C, 30 MPa	Fracture strength: ~750 MPa, wear loss: ~0.1 mg, Friction co efficient: ~0.6, % TD: >99	[24]
Mixture of boehmite derived alumina and α-Al_2O_3 seeds with 400 nm particle size	CVD-MWCNTs, 0.5 wt%, Φ: 20–30 nm, l: 20–30 μm	Sol gel processing, ultrasonication, mechanical stirring, ball milling	Uniaxial pressing, CIPing, sintering, 1600 °C, N_2, HIPing, 1300 °C, 200 MPa	K_{IC}: 5.5 ± 0.2 MPa $m^{1/2}$, H_v: 2150 ± 20 Kg/mm^2, % TD: 9 9.52 ± 0.05	Present work

Table 1 summarizes the various methods of making alumina–CNT composites along with their highest improvement in the mechanical properties. In most of the cases, consolidation was carried out by hot pressing [8,12] or by spark plasma sintering (SPS) [7,19] at temperatures ranging from 1150 °C to 1800 °C. Relative density > 99.5% was achieved by hot press technique at temperatures of about 1500 °C [13] whereas 100% theoretical density (TD) was achieved through SPS even at temperatures lower than 1150 °C [19]. Though appreciable densities were achieved using these sintering techniques, they have their own limitations with respect to the usage of bigger dies with complex shaping and the productivity. Moreover, the achievement of full densification depends not only on the consolidation technique but also on the other parameters such as purity of starting materials and their morphology, compositions, degree of dispersion of CNTs etc. Thus, the processing route starting from the choice of raw materials, method of dispersion and the densification affects density and hence the mechanical properties like strength and toughness of the composites.

Therefore, there is a need for an improved method to prepare composite powder having uniformly distributed CNTs followed by shaping and densification processes to provide larger, denser and complex shaped components with enhanced productivity. In the present study, alumina–CNT composite powder with homogeneous CNT distribution was prepared by aqueous sol gel process. The powder was further shaped by cold isostatic pressing followed by pressureless sintering and hot isostatic pressing (HIPing) as these techniques are well-suited for producing larger components with complicated structures. Moreover this method has better production rate compared to the hot pressing and SPS sintering techniques.

During powder preparation CNTs were first coated with boehmite sol to avoid CNT to CNT contact and to improve the matrix network. Alumina seeds were introduced prior to gelation in the coating process as they enhance α phase formation in sol gel alumina, sintering behaviour and densification [22]. MWCNTs were first dispersed in boehmite sol by ultra sonication in combination with magnetic stirring followed by high speed mechanical stirring for effective dispersion of CNTs. Alumina seeds in the form of slurry were added to the sol at this stage followed by gelation, drying and calcination. The calcined powders were compacted, sintered, hot isostatically pressed and characterized for their physical and mechanical properties.

2. Experimental procedure

Commercially available boehmite powder, high purity alumina and CVD synthesized multi wall carbon nano tubes (MWCNTs) were used as raw materials for this process. The characteristics of the starting materials as per the supplier's specifications are listed in Table 2.

2.1. Pre treatment of MWCNTs

5 g of the procured MWCNTs were calcined at 500 °C for 1 h in air to get rid of amorphous carbon. They were further refluxed with 6 molar nitric acid solutions at 70–80 °C for 60 min in a magnetic stirrer to remove the catalyst particles and to introduce functional groups on the surface of MWCNTs.

2.2. Preparation of boehmite sol

200 g of the procured boehmite powder having 77% alumina content was mixed with 800 g of deionized water in a high speed stirrer at ambient conditions for 30 min and the pH was adjusted to 2.5–3 by drops wise addition of nitric acid under constant stirring for 2 h. Mg $(NO_3)_2{\cdot}6H_2O$ (Sigma Aldrich, USA) was added as a sintering aid to the sol to give 500 ppm of MgO with respect to the final alumina content.

2.3. Preparation of alumina slurry

Alumina powder was made into slurry of 50% solid loading in water using Darvan821A (R.T. Vanderbilt Co., Inc., Norwalk, CT, USA) as a dispersant. This mixture was ball milled in a poly ethylene container for 12 h using alumina balls as a milling media and the resulting slurry was filtered and degassed under vacuum for 10–15 min.

2.4. Surface coating of MWCNTs, seeding and gelation

0.5 wt% of functionalized MWCNTs were dispersed in the boehmite sol using probe type ultra sonicator in combination with magnetic stirring. The use of magnetic stirring was preferred in combination with ultrasonication to mobilize the CNT clusters towards the sonication probe for efficient dispersion. The total quantity of boehmite sol and MWCNTs was divided into 10 parts and each part was sonicated for 15–20 min for achieving better dispersion. The parts of alumina sol dispersed with CNTs were finally mixed together under

Table 2
Characteristics of boehmite, alumina and MWCNT starting powder.

Charateristics	Disperal 20	Alumina	MWCNTs
Manufacturer	Sasol GmbH, Hamburg, Germany	A16SG, Almatis GmbH Giulinistrasse, Germany	Chemapol Industries, Mumbai, India
Particle size (d_{50})	30 μm	0.4 μm	Diameter – 20–30 nm Length – 20–30 μm
BET surface area	150 m^2/g	8.9 m^2/g	–
Chemical analysis (as per the supplier's list)	Al_2O_3 – 77%, Na_2O – 0.002% Fe_2O_3 – 0.01%, SiO_2 – 0.012%	Fe – 0.02%,Na_2O – 0.07% SiO_2 – 0.03%,CaO – 0.02%	Amorphous carbon – 2 wt% catalyst – 3 wt%

vigorous stirring conditions for 1 h using a high speed mechanical stirrer. The dispersion was carried out in two steps to enhance the dispersion of CNTs into the alumina sol. Alumina slurry having 50 wt% of solid content was seeded at this stage. The proportion of alumina from boehmite and from slurry was maintained in a ratio of 80:20 and the stirring was continued for another 1 h. According to Messing and Kumagai a quantity of 1–2 wt% alumina seeds was sufficient to enhance α-phase formation of alumina from boehmite [22,23]. However, a seed proportion of 20% is taken for this work to increase the proportion of micron sized particles in the finer sol gel alumina to enhance the particle packing factor. The sol containing uniformly distributed CNTs and seeds was gelled by adjusting the pH to 14–14.5 by drop wise addition of ammonia.

2.5. Preparation of alumina–CNT composites

The gel was dried at 80–90 °C in a hot air oven and calcined at 1000 °C for 1 h under vacuum. The calcined powder was milled in isopropyl alcohol medium for 1 h using alumina balls and dried at 60–70 °C. Samples were compacted uniaxially at 10–15 MPa followed by cold isostatic pressing at 200 MPa and sintered at 1400–1600 °C for 1 h in flowing nitrogen atmosphere. Samples that were sintered at 1600 °C were further isostatically hot pressed (HIPed) at 1300 °C for 2 h at 200 MPa

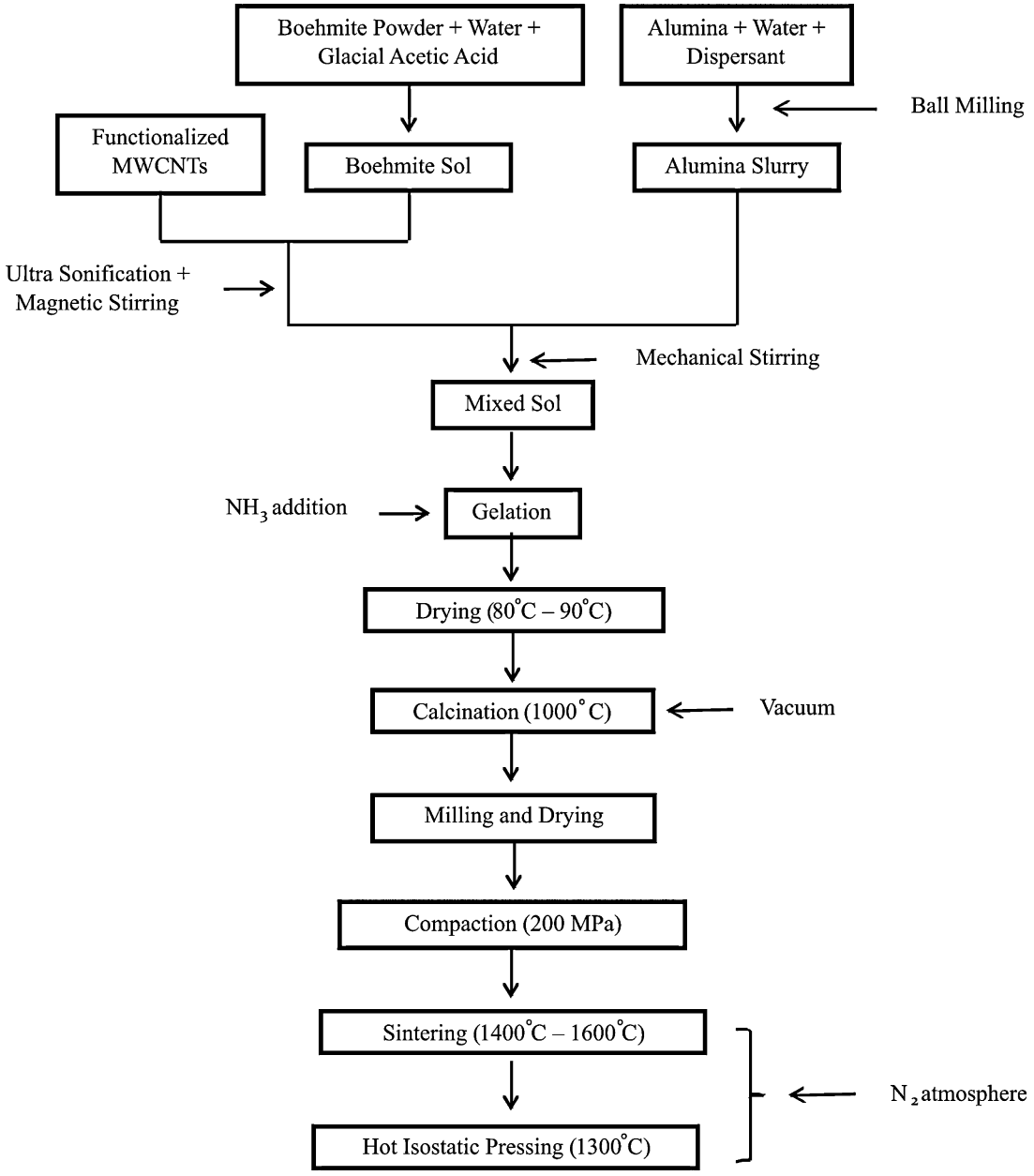

Fig. 1. Flow chart for the sol gel process for alumina–CNT composites.

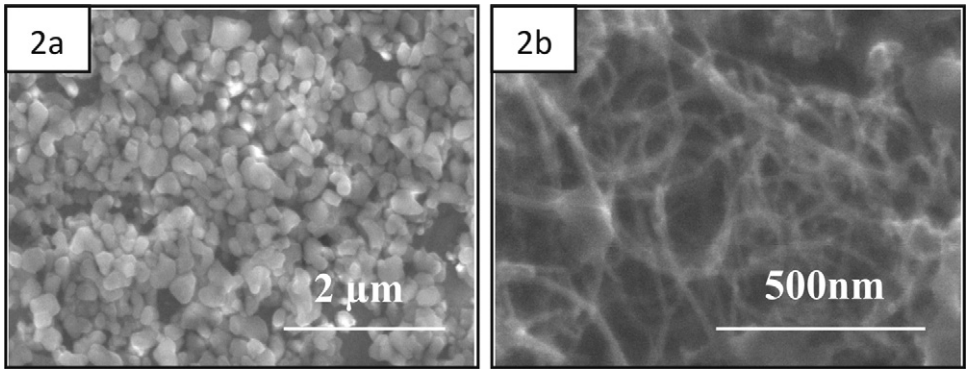

Fig. 2. Morphology of starting materials (a) alumina and (b) MWCNTs.

as they acquired 0% open porosity after pressureless sintering. The entire process is shown as a flowchart in Fig. 1

2.6. Characterization of alumina–CNT composites

Microstructures of alumina, MWCNTs and coating of alumina on the surface of CNTs and fractured and cracked microstructures of the sintered and HIPed composites were characterized by FESEM (Quanta 400, The Netherlands). Energy-dispersive X-ray spectroscopy (EDS) analysis (EDX TSL, Genesis, USA) was carried out on the calcined alumina CNT composite powder produced through the presented sol gel process to confirm the purity of the composites. Decomposition and phase transition of alumina from boehmite coated CNTs was identified by TGDSC. This was conducted in a nitrogen atmosphere to avoid peak formation due to loss of CNTs. Densities were measured by Archimedes principle and phase analyses were carried out by XRD (Philips, PWD, Model 1830, The Netherlands). Hardness was measured by Vickers (Leco, USA) indentation at 10 kg load and fracture toughness was calculated by the following Ansti's equation [24]:

$$K_{IC} = 0.016 \left(\frac{E}{H}\right)^{1/2} \left(\frac{P}{c^{3/2}}\right)$$

Where E is the Young's modulus and H is the Vickers hardness, P is the load and c is the crack length. Though there are arguments in evaluating K_{IC} using indentation method, it is still a reliable and economic method to evaluate the fracture toughness of the composites [5], especially when microstructural features the present reinforcement mechanisms such as pull out of CNTs, fracture of CNTs, crack bridging and crack deflections [21].

Further, the retention of CNTs in the composites after HIPing process was confirmed by Raman studies.

3. Results and discussion

Fig. 2 shows the morphology of alumina seeds (Fig. 2a) and MWCNTs (Fig. 2b). Alumina particles have sizes in the range of 300–400 nm and are free of agglomeration whereas the MWCNTs, with diameters in the range of 20–30 nm, are clustered together.

3.1. Thermal decomposition and phase transition of sol gel alumina

Fig. 3 shows the TGA and DSC curves of dried sol gel alumina powder contain 0.5 wt% MWCNTs. The initial weight loss at about 100 °C in the TGA curve corresponds to loss of the physically combined water and the remaining weight loss occurs by 700 °C. The endotherms at about 100 °C and 460 °C in the DSC pattern confirm the evaporation of free water and the formation of γ alumina respectively. The exotherm at about 1180 °C represents the transformation to α alumina. Therefore, the sol gel powder produced in the present process was calcined at 1000 °C, which is lower than the transformation temperature, to avoid the formation of hard agglomerates and to improve its sinterability.

3.2. Surface coating of MWCNTs

Fig. 4 compares the structure of MWCNTs before and after coating with sol gel alumina. It can be observed from Fig. 4b that the CNTs are homogeneously coated with alumina sol. Fig. 5 shows the XRD patterns of Alumina–MWCNT composite powder before calcination (Fig. 5a), calcined at 500 °C (Fig. 5b) and calcined at 1000 °C (Fig. 5c). Fig. 5a shows peaks corresponding to boehmite and alpha phase alumina which were used during sol preparation. Fig. 5b shows

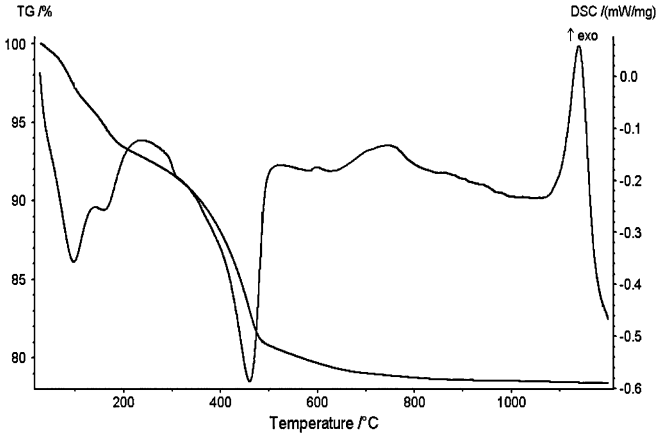

Fig. 3. TGA and DSC analysis of dried alumina sol gel powder containing 0.5 wt% MWCNTs.

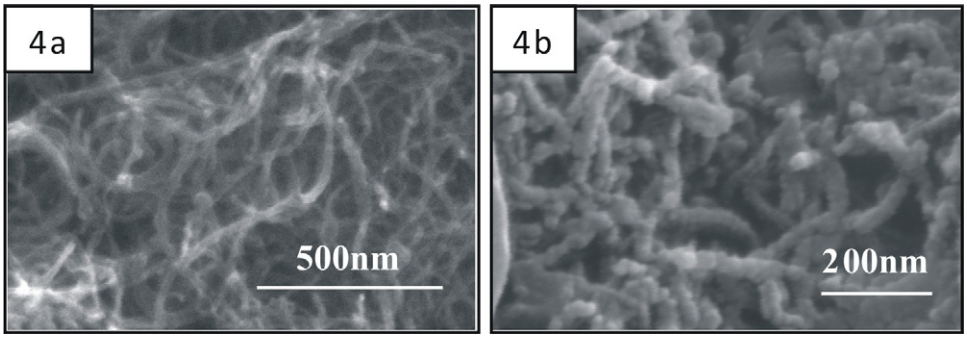

Fig. 4. Microstructure of MWCNTs (a) before and (b) after coating with alumina sol.

the intermediate phase transition of boehmite at 500 °C to form γ alumina prior to the complete phase transition to α alumina at 1000 °C as seen in Fig. 5c. The peaks corresponding to the MWCNTs are difficult to detect in all the patterns due to their lesser quantity compared to alumina. It can be observed that the phase transitions shown in XRD match well with the TGDSC curve in Fig. 3.

3.3. Physical and mechanical characterization

Fig. 6a shows the microstructure of the calcined alumina CNT composite powder produced by the presented aqueous sol gel process. It can be observed that the CNTs are well coated with sol gel alumina and dispersed in the alumina powder matrix. The purity of the synthesized composite powder was further checked using EDS (Fig. 6b) where only the peaks that correspond to Al, O and C were observed. The peaks that correspond to carbon are not so visible possibly due to the lower concentration of carbon with respect to Al and O content. The peak corresponding to Au is present due to the gold sputtering process conducted on the samples prior to FESEM and EDS analysis.

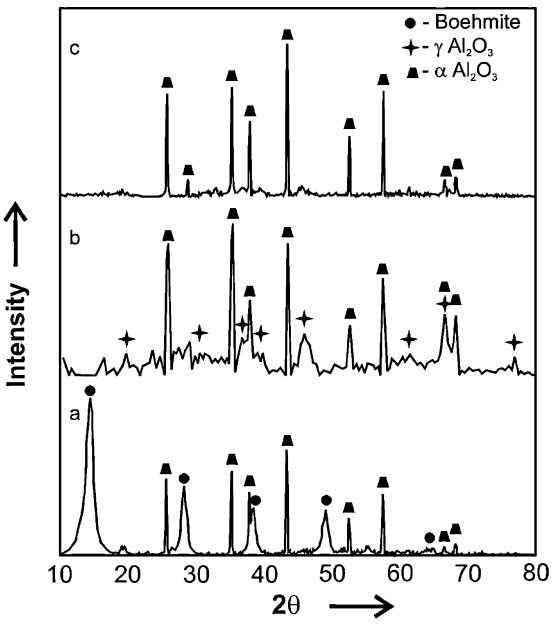

Fig. 5. XRD of sol gel alumina and MWCNTs composite powder (a) before and (b) after calcination at 1000 °C.

Fig. 7 shows the fractured surface of composites containing 0.5 wt% MWCNTs sintered at 1400 °C (Fig. 7a), 1500 °C (Fig. 7b) and 1600 °C (Fig. 7c) for 1 h. The micrograph shows the evolution of densification and grain growth of the composites with increasing sintering temperature. The grain sizes ranging from 250 nm to 550 nm observed for the samples sintered at 1400 °C increased to 500 nm to 1.5 μm for the samples sintered at 1600 °C. Fig. 7d shows the thermally etched microstructure of alumina with 0 wt% MWCNTs sintered at 1400 °C for 1 h. The degree of densification and the grain sizes are not same for the pure alumina (Fig. 7d) and the composite with 0.5 wt% MWCNTs (Fig. 7a) at though they are sintered at the same temperature. The grain size of pure alumina ranges from 0.8 to 1.2 μm whereas the grain size of alumina in the composite is in the range of 250–550 nm after the sintering at 1400 °C. This is attributed to the role of the MWCNTs in inhibiting the grain growth. Moreover, dense microstructure (>96% TD) is achieved in case of pure alumina whereas the microstructure of the composite is still porous showing density less than 85% of TD at 1400 °C. To obtain materials with improved mechanical properties, it is not only necessary to retain the microstructure with smaller grain size but it also needs to be accompanied with minimum porosity, which are generally not very easy to achieve while fabricating the CNT based composites. However, these aspects have been achieved in the alumina CNT composites prepared by the present processing route at 1600 °C (Fig. 7c). The composites show no open porosity and the grain size is less than 1.5 μm after sintering at 1600 °C for 1 h.

Fig. 8 shows the density data for sol gel derived alumina–MWCNT composite samples sintered at 1400 °C, 1500 °C and 1600 °C. The density increases with temperature and values of about 99.3% and 96.5% of the TD are attained for the composites with 0 wt% and 0.5 wt% MWCNTs respectively at 1600 °C. Samples that contain 0.5 wt% MWCNTs and sintered at 1600 °C were subjected to hot isostatic pressing (HIPing) as it had zero percent open porosity. HIPing was carried out to eliminate the residual porosity and to improve the mechanical characteristics. For sake of comparison, the sample containing 0 wt% CNTs sintered at 1600 °C was also subjected to HIPing along with the composite sample. The elimination of internal voids during this process enhances the density of 0.5 wt%

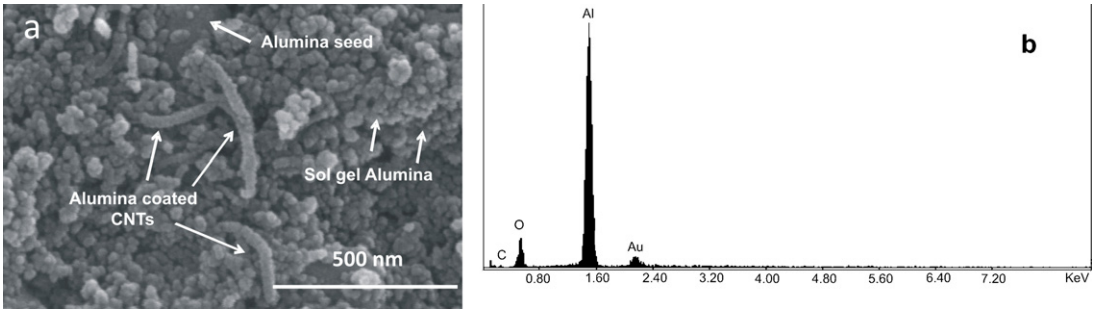

Fig. 6. Microstructure (a) and the EDS analysis (b) of calcined alumina CNT composite powder.

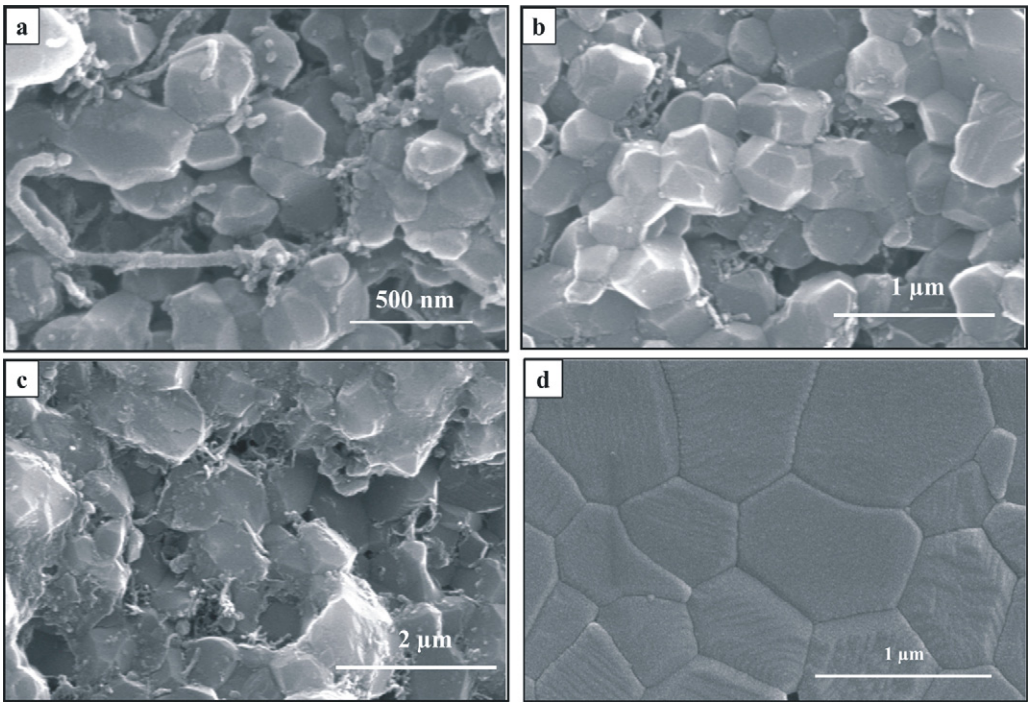

Fig. 7. Composites containing 0.5 wt % MWCNTs and sintered at (a) 1400 °C (b) 1500 °C (c) 1600 °C and (d) alumina with 0 wt % MWCNTs and sintered at 1400 °C.

MWCNTs–alumina composite from 96.5% TD to 99.52% TD while the pure alumina sample attains 100% TD.

Fig. 9a shows the polished and thermally etched surface of the HIPed sample. It is a known phenomenon that the CNTs situated at the inter-granular sites improve the fracture toughness as they hinder and deflect the crack propagation in the matrix, while the CNTs present in the intra-granular sites improve the strength and toughness through grain bridging. It can be observed from Fig. 8a that the CNTs are uniformly distributed both at inter and intra granular sites of the closed packed matrix .The distribution of CNT reinforcements at these sites enhances the intrinsic mechanical properties of the matrix material through crack deflection and grain bridging. Fig. 9b shows the fracture microstructure of the HIPed sample. It can be noticed that the pullouts of CNTs are present both at the grain boundaries and in the grains. The pullouts are longer at the grain boundary sites compared to the CNTs located inside the grains. This shows that the fracture of the composite occurred due to the fracture of grain boundaries (inter-granular)

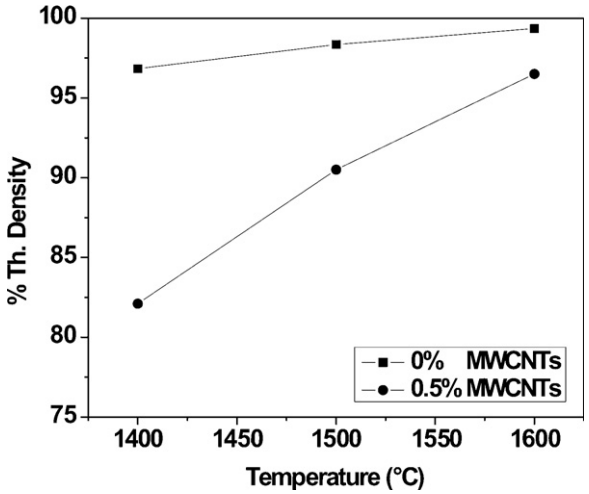

Fig. 8. Plot of sintered TD with temperature for composites processed with 0 and 0.5 wt% of MWCNTs.

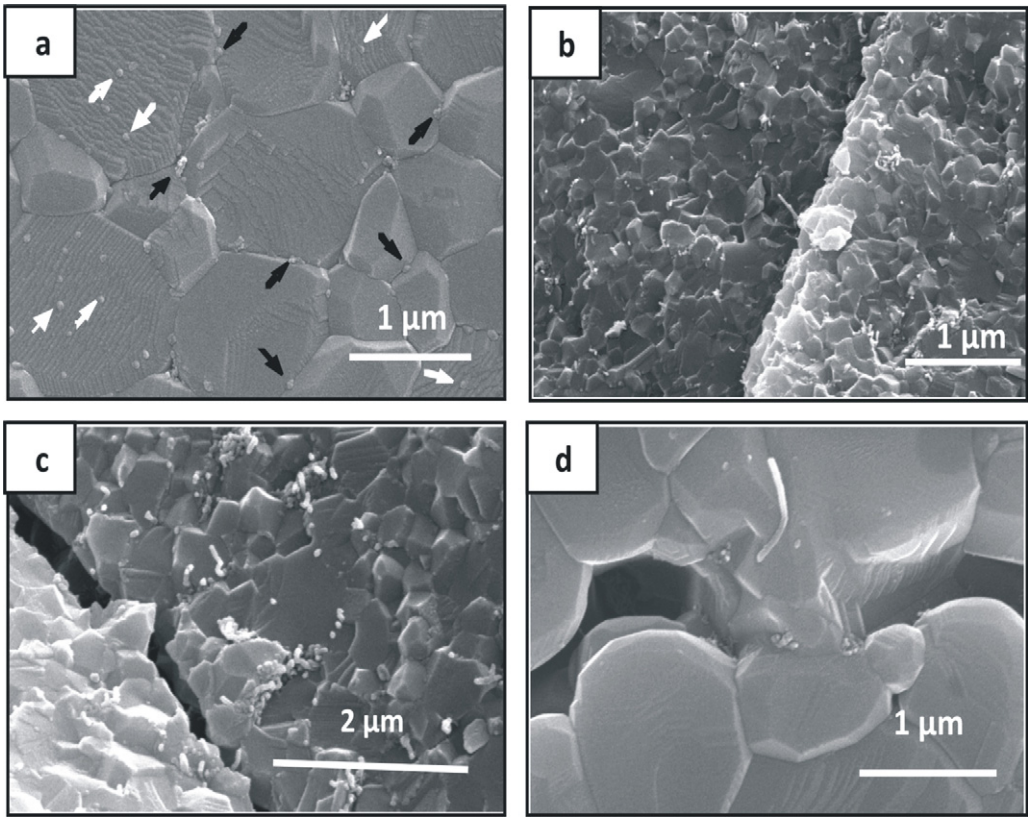

Fig. 9. Microstructure of HIPed composite (a) polished and thermally etched surface (b) fractured surface (c) crack propagation (d) grain bridging due to CNTs.

and grains (trans-granular) of alumina together with the fracture of reinforced CNTs. This provides evidence for the sharing of the fracture stress of the composite by the CNTs and hence its reinforcing effect. Moreover, uniform distribution of CNTs in the fractured surface proves the effectiveness of the dispersion by ultra sonication in combination with magnetic stirring followed by high speed mechanical stirring. Also, the gelation of the dispersed CNTs helps in improving the dispersion of CNTs by arresting their re-agglomeration and settling within the sol. Hence the level of dispersion and the processing route play a very important role in improving the mechanical properties of CNT based composites. The mechanical properties can be improved by increasing the level of dispersion of CNTs in the matrix. The effect of processing route on the mechanical properties of CNT–alumina composites was studied by Lim et al. [25] and the results show that the reduction in CNT agglomeration during the tape casting process contributed to the improvement in densification and other mechanical properties. The present dispersion technique results in homogeneous distribution of CNTs in the alumina matrix and contributes to the overall improvement in densification and improvement in the mechanical properties.

Fig. 9c and d show the crack deflection and grain bridging that have occurred in the composites. As discussed above, these mechanisms are important in achieving composites with improved mechanical characteristics. Fig. 10 shows the Raman spectra of MWCNTs (Fig. 10a), HIPed alumina (Fig. 10b) and HIPed alumina–CNT composite body (Fig. 10c). The MWCNTs spectrum in Fig. 10a shows the D, G and G′ peaks at 1350 cm^{-1}, 1580 cm^{-1} and 2650 cm^{-1} respectively. The IG/ID ratio, an index of the quality of CNTs was 1.17 showing that the CNTs are well graphitized. The D peak is associated with

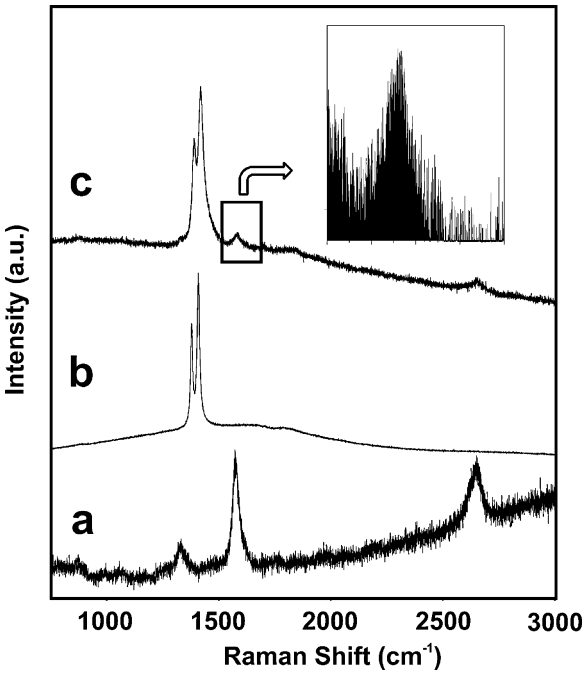

Fig. 10. Raman spectrum of (a) MWCNTs (b) HIPed alumina (c) HIPed alumina CNT composite body.

Table 3
Properties of the sintered and HIPed samples containing 0 wt% and 0.5 wt% of MWCNTs.

Properties	Alumina sintered at 1600 °C	Composite sintered at 1600 °C	HIPed alumina	HIPed composite
% TD	99.30	96.50	100	99.52
Hardness V_{HN} 10 Kg load (Kg/mm^2)	1850 ± 20	1975 ± 30	2000 ± 10	2150 ± 20
Fracture toughness (MPa m$^{1/2}$)	3.0 ± 0.2	4.1 ± 0.1	4.2 ± 0.3	6.5 ± 0.2

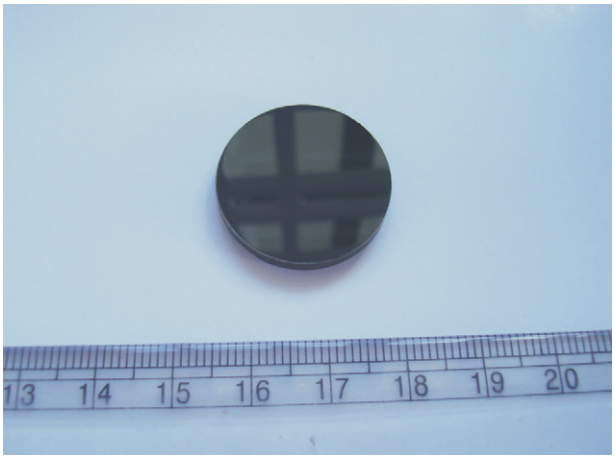

Fig. 11. HIPed and polished alumina MWCNT composite.

the disorder of CNT structure and the G peak is related with the C–C stretching mode of CNTs representing their crystalline order. A shoulder can be observed on the right side of the G-peak which is a characteristic feature of MWCNTs. Fig. 10b shows the characteristic Raman peaks of alumina at 1373 cm^{-1} and 1403 cm^{-1} and Fig. 10c shows the characteristic peaks of alumina along with that of the MWCNTs in the HIPed sample. The intensity of the peaks corresponding to MWCNTs appears to be lower when compared to those of alumina due to the lower concentration of the former. The D peak can be observed adjacent to the alumina peak almost merged with it and the G peak can be observed at 1580 cm^{-1}. The G peak of MWCNTs in the HIPed sample displays a shoulder on the right side indicating the retention of the structure of CNTs after undergoing the fabrication steps including HIPing at 1300 °C. The magnified view of the G peak is darkened to provide a better observation of the shoulder. Fig. 11 shows the HIPed and polished composite sample prepared by the present process. Table 3 shows the properties of the sintered and HIPed samples containing 0 wt% and 0.5 wt% of MWCNTs. As discussed in the earlier sections, the density of the pure alumina sample increased from 99.3% TD to 100% TD after HIPing and the composite density increased from 96.5% TD to 99.52% TD. The sintered composite body showed improved hardness values (1975 Kg/mm^2) compared with the pure alumina body (1850 Kg/mm^2) and both values of hardness further improved to 2000 Kg/mm^2 and 2150 Kg/mm^2 respectively after HIPing. A similar trend is indicated in case of fracture toughness with better toughness for the sintered composite body (4.10 MPa m$^{1/2}$) compared to the pure alumina body (3.0 MPa m$^{1/2}$), which further increases to 3.6 MPa m$^{1/2}$ in case of pure alumina and to 5.5 MPa m$^{1/2}$ in case of the composite after HIPing.

4. Conclusion

Here an attempt has been made to demonstrate through sol gel method, the process of making alumina and MWCNT reinforced composites. The effective dispersion of CNTs was achieved by ultrasonification in combination with magnetic stirring followed by high speed mechanical stirring. The process conditions for shaping, sintering and HIPing to achieve a product with TD greater than 99.5% have been demonstrated. The density, hardness and fracture toughness of the composite were measured and CNT retention in the composites after HIPing was verified using Raman spectroscopy. The microstructural examination of the fracture surfaces confirmed the reinforcing effect of CNTs in the alumina matrix by crack bridging and CNT pull out mechanism. This study also exhibits the procedure for making composites with a hardness of 2150 ± 20 (Kg/mm^2) and a fracture toughness of 5.5 ± 0.2 MPa m$^{1/2}$.

References

[1] S. Iijima, Structural flexibility of carbon nano tubes, J. Chem. Phys. 104 (1996) 2089–2092.
[2] K.E. Thomson, D.T. Jiang, R.O. Ritchie, A.K. Mukherjee, A preservation of carbon nanotubes in alumina-based nanocomposites via Raman spectroscopy and nuclear magnetic resonance, Appl. Phys. A 89 (2007) 651–654.
[3] S.W. Kim, W.S. Chung, K. Sohn, C.Y. Son, S. Lee, Improvement of flexure strength and fracture toughness in alumina matrix composites reinforced with carbon nanotubes, Mater. Sci. Eng. A 517 (2009) 293–299.
[4] K. Ahmad, W. Pan, Dramatic effect of multiwalled carbon nanotubes on the electrical properties of alumina based ceramic nanocomposites, Compos. Sci. Technol. 69 (2009) 1016–1021.
[5] D. Jiang, K. Thomson, J.D. Kuntz, J.W. Ager, A.K. Mukherjee, Effect of sintering temperature on a single-wall carbon nanotube-toughened alumina-based nano composite, Scripta Mater. 56 (2007) 959–962.
[6] Ch. Laurent, A. Peigney, O. Dumortier, A. Rousset, Carbon nanotubes–Fe–Alumina nanocomposites. Part II: microstructure and mechanical properties of the hot-pressed composites, J. Eur. Ceram. Soc. 18 (1998) 2005–2013.
[7] C.N. He, F. Tian, S.J. Liu, A carbon nanotube/alumina network structure for fabricating alumina matrix composites, J. Alloys Compd. 478 (2009) 816–819.
[8] J.W. An, D.H. You, D.S. Lim, Tribological properties of hot-pressed alumina–CNT composites, Wear 255 (2003) 677–681.
[9] J. Sun, L. Gao, X. Jin, Reinforcement of alumina matrix with multi-walled carbon nanotubes, Ceram. Int. 31 (2005) 893–896.
[10] S.I. Cha, K.T. Kim, K.H. Lee, C.B. Mo, S.H. Hong, Strengthening and toughening of carbon nanotube reinforced alumina nano composite fabricated by molecular level mixing process, Scripta Mater. 53 (2005) 793–797.
[11] C.B. Mo, S.I. Cha, K.T. Kim, K.H. Lee, S.H. Hong, Fabrication of carbon nanotube reinforced alumina matrix nanocomposite by sol–gel process, Mater. Sci. Eng. A 395 (2004) 124–128.

[12] Y. Guo, H. Cho, D. Shi, J. Lian, Y. Song, J. Abot, B. Poudel, Z. Ren, L. Wang, R.C. Ewing, Effects of plasma surface modification on interfacial behaviors and mechanical properties of carbon nanotube–Al_2O_3 nanocomposites, Appl. Phys. Lett. 91 (2007) 261903.

[13] S. Bi, G. Hou, X. Su, Y. Zhang, F. Guo, Mechanical properties and oxidation resistance of α-alumina/multi-walled carbon nanotube composite ceramics, Mat. Sci. Eng. A 528 (2011) 1596–1601.

[14] A.C. Zaman, C.B. Ustundag, A. Celik, A. Kara, F. Kaya, C. Kaya, Carbon nanotube/boehmite-derived alumina ceramics obtained by hydrothermal synthesis and spark plasma sintering (SPS), J. Eur. Ceram. Soc. 30 (2010) 3351–3356.

[15] G. Yamamoto, M. Omori, K. Yokomizo, T. Hashida, Mechanical properties and structural characterization of carbon nanotube/alumina composites prepared by precursor method, Diamond Relat. Mater. 17 (2008) 1554–1557.

[16] J.P. Fan, D.Q. Zhao, M.S. Wu, Z.N. Xu, J. Song, Preparation and microstructure of multi-wall carbon nanotubes-toughened Al_2O_3 composite, J. Am. Ceram. Soc. 89 (2006) 750–753.

[17] I. Ahmad, M. Unwin, H. Cao, H. Chen, H. Zhao, A. Kennedy, Y.Q. Zhu, Multi-walled carbon nanotubes reinforced Al_2O_3 nanocomposites: mechanical properties and interfacial investigations, Compos. Sci. Technol. 70 (2010) 1199–1206.

[18] S.C. Zhang, W.G. Fahrenholtz, G.E. Hilmas, E.J. Yadlowsky, Presureless sintering of carbon nanotube–Al_2O_3 composites, J. Eur. Ceram. Soc. 30 (2010) 1373–1380.

[19] G.D. Zhan, J.D. Kuntz, J. Wan, A.K. Mukherjee, Single-wall carbon nanotubes as attractive toughening agents in alumina-based nanocomposites, Nat. Mater. 2 (2003) 38–42.

[20] M. Estili, A. Kawasaki, An approach to mass-producing individually alumina-decorated multi-walled carbon nano tubes with optimized and controlled compositions, Scripta Mater. 58 (2008) 906–909.

[21] T. Wei, Z. Fan, G. Luo, F. Wei, D. Zhao, J. Fan, The effect of carbon nanotubes microstructures on reinforcing properties of SWNTs/alumina composite, Mar. Pollut. Bull. 43 (2008) 2806–2809.

[22] G.L. Messing, M. Kumagai, Low-temperature sintering of α-Al_2O_3-seeded boehmite gel, Am. Ceram. Soc. Bull. 73 (1994) 88–93.

[23] M. Kumagai, G.L. Messing, Enhanced densification of boehmite–sol–gels by α-alumina seeding, Comm. Am. Ceram. Soc. 67 (1984) C230–C231.

[24] G.R. Anstis, P. Chantiklul, B.R. Lawn, D.B. Marshall, A critical evaluation of indentation techniques for measuring fracture toughness: I Direct crack measurements, J. Am. Ceram. Soc. 64 (1981) 533–538.

[25] D.S. Lim, D.H. You, H.J. Choi, S.H. Lim, H. Jang, Effect of CNT distribution on tribological behavior of alumina–CNT composites, Wear 259 (2005) 539–544.